EPR Studies of the "EPR Nondetectable" Met Derivative of Hemocyanin: Perturbations and Displacement of the Endogenous Bridge in the Coupled Binuclear Copper Active Site

Dean E. Wilcox, John R. Long, and Edward I. Solomon*

Contribution from the Department of Chemistry, Massachusetts Institute of Technology, Cambridge, Massachusetts 02139, and the Department of Chemistry, Stanford University, Stanford, California 94305. *Received June 9, 1983*

Abstract: The broad, weak EPR signals associated with met hemocyanin have been shown to originate from a small fraction of the sites where the endogenous bridge has a lower stability constant and can be uncoupled at low pH through competitive displacement by specific exogenous anions. This results in zero-field-split triplet EPR signals of the dipolar interacting cupric ions where bridging exogenous ligands determine the Cu(II)–Cu(II) separation, thus modifying these EPR signals. The heterogeneous sites that exhibit this behavior, however, are not damaged sites as they can be regenerated to function normally in reversible oxygen binding when the endogenous bridge is present at high pH. Therefore, the intrinsic pK_a (>7) exhibited by the endogenous bridge in these sites represents this value in all hemocyanin sites and eliminates low-pK_a possibilities (e.g., carboxylate) for this protonatable residue. The competitive anion binding behavior of these unique sites has also provided insight about the stability constant of the endogenous bridge. Finally, this study provides clear evidence for distinctly different endogenous and exogenous bridging positions in the coupled binuclear copper active site.

A coupled binuclear copper active site[1] exists in a variety of proteins and enzymes that perform many different biological functions. Hemocyanin, which reversibly binds dioxygen as peroxide during its role of oxygen transport in arthropods and molluscs, has served as a prototype in recent studies[2-6] of this general class of metalloprotein sites. In order to elucidate this EPR-silent binuclear cupric unit, derivatives of the hemocyanin active site have been chemically prepared and subjected to detailed spectroscopic examination. From these studies has emerged the spectroscopically effective oxy hemocyanin active site[1,3] pictured in Figure 1. Two tetragonal cupric ions are superexchange coupled by an equatorial endogenous bridge (RO−) while the exogenous anion peroxide also equatorially bridges in a μ-1,2 geometry.

Two of the hemocyanin derivatives, met and dimer, have a binuclear cupric site and have proven especially important in probing the role of the endogenous bridge.[1,4] Dimer is prepared[7] by NO + O_2 oxidation of deoxy and exhibits (Figure 2A) an EPR signal with an intense broad feature at $g \simeq 2$ and a weak feature at $g \simeq 4$. This signal, which corresponds to ~65%[7b] of the sites and exhibits negligible exchange coupling ($|2J| < 5$ cm^{-1}), has been simulated[8] and shown to correspond to two dipolar interacting tetragonal copper(II)'s held ~6 Å apart. Addition of excess azide[4] results in the dimer N_3^- form which exhibits a new but similar EPR signal (Figure 2A), indicating retention of the same site structure, but with a change in Cu–Cu separation to ~5 Å. Dialysis of either dimer form produces the met derivative.[4] Met is normally prepared by two-electron oxidation of deoxy[9] or associative ligand displacement of peroxide from oxy.[10] Greater than 90% of the sites in met are EPR nondetectable,[4] paralleling the EPR nondetectability of oxy.

A comparison[1,3] of the ligand-field optical spectra of dimer and met has demonstrated that the individual tetragonal cupric energy levels of met are not significantly perturbed by the interaction between the ions which eliminates the paramagnetism (EPR signal). This result strongly indicates that a weak interaction due to antiferromagnetic coupling mediated by a bridging ligand superexchange pathway is responsible for the lack of EPR signals in met and oxy. Magnetic susceptibility (SQUID) measurements[11] on oxy, in fact, have indicated that a paramagnetic triplet spin state would be >550 cm^{-1} higher in energy than the singlet. This requires that the endogenous bridging ligand provide an efficient pathway for this relatively strong superexchange coupling. The preparation of dimer hemocyanin produces a metastable form of the site where the endogenous bridge is broken by certain bridging exogenous anions which keep the coppers $\gtrsim$5 Å apart. The resulting EPR signals are those from the dipolar interacting Cu(II)'s of the dimer site. Removal of these "group 2"[2] exogenous anions allows the bridge to re-form; the dimer EPR signals disappear as the sites are converted to met.

Even though met is EPR nondetectable, weak signals[4,12] at $g \simeq 2$ and $g > 4$ are associated with this derivative. This spectrum is shown at low temperature and high sensitivity in Figure 2B. While the $g \simeq 2$ signal originates from $\lesssim$3% of the sites, it is difficult to quantify the broad, weak signal most obvious at $g > 4$. A key experiment,[4] however, has shown that all the EPR signals associated with met must originate from <10% of the met sites. Mollusc met hemocyanin can be regenerated to oxy[9] by small excesses of peroxide. When *Busycon* met is regenerated with peroxide to >90% EPR-nondetectable oxy sites, the EPR spectrum is not affected (Figure 2B). Unfortunately, these EPR signals associated with met have led to confusion about the nature of this derivative and, in particular, a misleading correlation[12,13] with

(1) Solomon, E. I. "Copper Proteins"; Spiro, T. G., Ed.; Wiley: New York, 1981; Chapter 2.
(2) (a) Himmelwright, R. S.; Eickman, N. C.; Solomon, E. I. *Biochem. Biophys. Res. Commun.* **1978**, *81*, 237–242. (b) Himmelwright, R. S.; Eickman, N. C.; Solomon, E. I. *Biochem. Biophys. Res. Commun.* **1978**, *81*, 243–247. (c) Himmelwright, R. S.; Eickman, N. C.; Solomon, E. I. *Ibid.* **1978**, *84*, 300–305. (d) Himmelwright, R. S.; Eickman, N. C.; Solomon, E. I. *J. Am. Chem. Soc.* **1979**, *101*, 1576–1586.
(3) Eickman, N. C.; Himmelwright, R. S.; Solomon, E. I. *Proc. Natl. Acad. Sci. U.S.A.* **1979**, *76*, 2094–2098.
(4) Himmelwright, R. S.; Eickman, N. C.; Solomon, E. I. *Biochem. Biophys. Res. Commun.* **1979**, *86*, 628–634.
(5) Hepp, A. F.; Himmelwright, R. S.; Eickman, N. C.; Solomon, E. I. *Biochem. Biophys. Res. Commun.* **1979**, *89*, 1050–1057.
(6) Himmelwright, R. S.; Eickman, N. C.; LuBien, C. D.; Solomon, E. I. *J. Am. Chem. Soc.* **1980**, *102*, 5378–5388.
(7) (a) Schoot Uiterkamp, A. J. M. *FEBS Lett.* **1972**, *20*, 93–96. (b) van der Deen, H.; Hoving, H. *Biochemistry* **1977**, *16*, 3519–3525.
(8) Schoot Uiterkamp, A. J. M.; van der Deen, H.; Berendsen, H. C. J.; Boas, J. F. *Biochim. Biophys. Acta* **1974**, *372*, 407–425.
(9) Felsenfeld, G.; Printz, M. P. *J. Am. Chem. Soc.* **1959**, *81*, 6259–6264.
(10) Witters, R.; Lontie, R. *FEBS Lett.* **1975**, *60*, 400–403.
(11) (a) Solomon, E. I.; Dooley, D. M.; Wang, R. H.; Gray, H. B.; Cerdonio, M.; Mogno, F.; Romani, G. L. *J. Am. Chem. Soc.* **1975**, *98*, 1029–1031. (b) Dooley, D. M.; Scott, R. A.; Ellinghaus, J.; Solomon, E. I.; Gray, H. B. *Proc. Natl. Acad. Sci. U.S.A.* **1978**, *75*, 3019–3022.
(12) Witters, R.; DeLey, M.; Lontie, R. "Structure and Function of Haemocyanin"; Bannister, J. V., Ed.; Springer-Verlag: Berlin, 1977; pp 239–244.

0002-7863/84/1506-2186$01.50/0

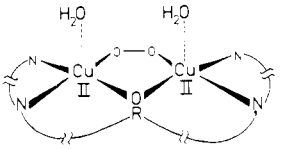

Figure 1. Spectroscopically effective oxy hemocyanin active site.

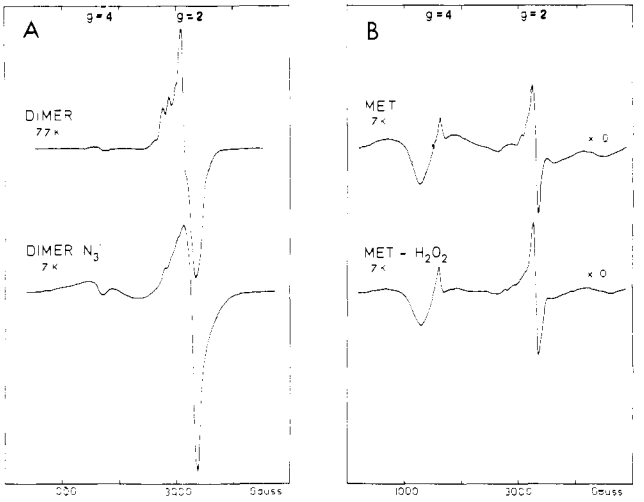

Figure 2. EPR spectra: (A) Dimer hemocyanin (77 K) and dimer + excess azide (7 K); ~3 mM protein. (B) Met hemocyanin and met + 10-fold excess H_2O_2 (7 K); 1 mM protein in 0.1 M acetate, pH 5.0.

dimer. Although the $g \gtrsim 4$ regions of both EPR spectra (Figure 2A,B) have some similarities, the relative magnitude of the $g \simeq 2$ region clearly indicates the signals are quite different. Further, quantification of these signals has indicated that most of the sites ($\gtrsim$65%) react to give the dimer signal while the met EPR signals originate from only $\lesssim$10% of the sites.

We report here our study of the EPR signals associated with met hemocyanin. While these signals are shown to originate from a heterogeneous fraction ($\lesssim$10%) of the met sites, these sites can, under certain conditions, be regenerated to oxy, thus showing that they are valid protein units capable of reversible oxygen binding. This study has revealed considerable information about the nature of the superexchange-mediating endogenous bridge and provides evidence for distinct endogenous and exogenous bridging positions at the coupled binuclear copper site.

Experimental Section

Hemocyanin was obtained from *Busycon canaliculatum* and *Lunatia heros* by foot puncture, from *Limulus polyphemus* by heart puncture, and from *Cancer borealis* and *Cancer magister* by removal of several legs. *Busycon*, *Lunatia*, and *Limulus* hemolymph was centrifuged and the hemocyanin pellet resuspended in buffer; hemolymph of the *Cancers* was dialyzed against buffer at 4 °C.

Mollusc met hemocyanin was prepared[10] by 37 °C incubation of oxy at pH 5.0 with 100-fold excess F^- or N_3^- for 48 h. Arthropod met was formed[9] by oxidation of deoxy with 10-fold excess H_2O_2 at pH 6.3 followed by dialysis to remove excess peroxide. The relative percentage of met and oxy was quantified by monitoring the 345-nm peroxide-to-copper charge-transfer intensity.

The heterogeneous fractions of *Limulus* hemocyanin were isolated according to a modified form of the procedure of Brenowitz et al.[14]

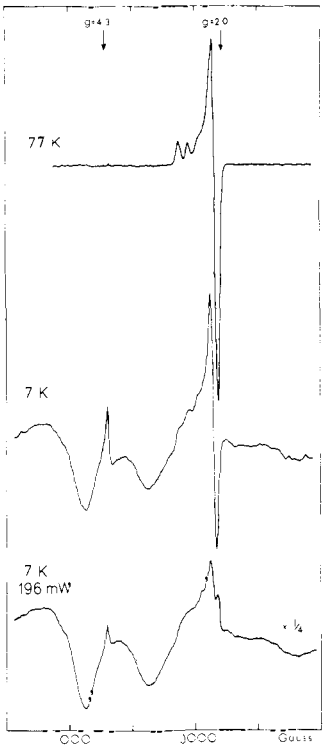

Figure 3. Met EPR spectrum (1 mM protein in 0.1 M acetate, pH 5.5) at 77 and 7 K (10- and 196-mW power).

Stripping buffer (20 mM Tris–glycine, 10 mM EDTA, pH 8.9) was used to deaggregate the protein and elution with a 0.17 to 0.40 M Cl^- buffered gradient on a 1.8 × 50 cm DEAE Sephacel column separated the five major fractions.

Ligand substitution reactions were performed by dialysis against appropriately buffered anion solutions at 4 °C. Regeneration of mollusc met to oxy was accomplished by treatment with 10-fold excess H_2O_2 followed by dialysis to remove excess peroxide. The following buffers (0.1 M) were used in the appropriate pH ranges: succinate, pH 3.5–5.5; acetate, pH 4.0–6.0; MES, pH 5.5–6.5; phosphate, pH 5.7–7.0; and Tris, pH >7.0.

EPR spectra were recorded at 100-kHz modulation and 20-G modulation amplitude on a Brüker ER 200D-SRC spectrometer and a Varian E-9 spectrometer; unless otherwise noted, 10-mW incident power was used and resonance conditions were typically 9.27 GHz at 77 K and 9.45 GHz at 7 K. Sample temperatures below 77 K were obtained with an Air Products LTD-3-110 Heli-Tran liquid helium transfer refrigerator. Optical spectra were recorded on Cary 14 and 17 recording spectrometers at room temperature.

All experimental EPR spectra shown, with the exception of Figure 11, are of the mollusc *Busycon*. The $g \simeq 2$ signal was quantified by double integration and comparison to the double integrated signal intensity of a $CuSO_4$ sample (50% glycerol) of known concentration. The relative intensity of the broad signals was quantified by the maximum to minimum height in the g = 5–8 region (700–1500 G). The sharp EPR signal of an iron impurity at g = 4.3 was found in all spectra with $T < 77$ K. Broad signals from condensed oxygen with features at g = 4.8, 1.6, and 1.3 were occasionally seen at liquid helium temperatures.

Computer simulations were performed with the program GNDIMER obtained from Prof. John Pilbrow at Monash University, Clayton, Victoria, Australia. The singlet–triplet splitting ($2J$) was determined with a least-squares fit of the temperature dependence of the broad signal intensity (I) using the Bleaney–Bowers[15] equation:

$$I = \frac{m}{T(3 + e^{-2J/kT})} \quad (1)$$

Results and Discussion

1. Physical Perturbations. The intensities of the EPR features associated with mollusc met hemocyanin depend on both temperature and microwave power as shown in Figure 3. At 77 K only a weak signal corresponding to $\lesssim$3% of the copper is observed

(13) (a) Verplaetse, J.; van Tornout, P.; Defreyn, G.; Witters, R.; Lontie, R. *Eur. J. Biochem.* **1979**, *95*, 327–331. (b) Rupp, H.; Verplaetse, J.; Lontie, R. *Z. Naturforsch., C* **1980**, *35*, 188–192. (c) Verplaetse, J.; Declercq, P.; Deleersnijder, W.; Witters, R.; Lontie, R. In "Invertebrate Oxygen Binding Proteins"; Lamy, J.; Lamy, J., Eds.; Dekker: New York, 1981; pp 589–596. (d) Witters, R.; Verplaetse, J.; Lijnen, H. R.; Lontie, R. "Invertebrate Oxygen Binding Proteins"; Lamy, J.; Lamy, J., Eds.; Dekker: New York, 1981; pp 597–602. (e) Lontie, R.; Gielens, C.; Groeseneken, D.; Verplaetse, J.; Witters, R. In "Oxidases and Related Redox Systems"; King, T. E. et al., Eds.; Pergamon: Oxford, 1982; pp 245–261. (f) Lontie, R.; Groeseneken, D. R. "Topics in Current Chemistry"; Boschke, F. L., Ed.; Springer-Verlag: Berlin, 1983; Vol. 108, pp 1–33.

(14) Brenowitz, M.; Bonaventura, C.; Bonaventura, J.; Gianazza, E. *Arch. Biochem. Biophys.* **1981**, *210*, 748–761.

(15) Bleaney, B.; Bowers, K. D. *Proc. R. Soc. (London), Ser. A* **1952**, *214*, 451–465.

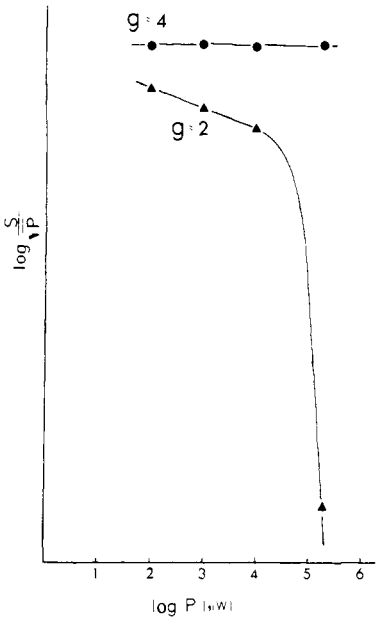

Figure 4. Power (P) saturation curves at 7 K for the $g \simeq 2$ (▲) and broad (●) met EPR signal intensity (S) measured as peak-to-peak heights at $g \approx 2$ and in the $g > 4$ region, respectively.

at $g \simeq 2$. As the temperature is lowered, at constant microwave power, the $g \simeq 2$ feature begins to saturate and a broad EPR signal extending from 0 to ~5000 G grows in intensity.[16] When the microwave power is increased (Figure 3, bottom) at the lowest accessible temperature, the $g \simeq 2$ signal is quite saturated relative to the broad signal, most clearly observed at $g > 4$.

Figure 4 quantifies the different relaxation[18] properties of these two signals. The broad signal shows at most only weak saturation at the highest accessible microwave power while the $g \simeq 2$ signal exhibits strong saturation characterized by $P_{1/2}$ on the order of 80 mW. While this saturation behavior could relate to different transition probabilities of one paramagnetic center, the entire broad signal (0 to ~5000 G) exhibits temperature and microwave power dependence which is distinctly different from that of the much narrower feature at $g \simeq 2$. Further, chemical perturbations (section 2) modify only the broad signal, confirming that these are distinct signals originating from different EPR-detectable centers. The ≲3% mononuclear cupric EPR signal at $g \simeq 2$ is due to sites that are irreversibly damaged during the met preparative procedure[19] and are not considered further. The broad EPR signal (Figure 3, bottom) associated with met, however, is the major focus of this study as it provides considerable insight into the coupled binuclear copper site.

The temperature dependence of the broad EPR signal intensity follows Curie law behavior ($I \propto 1/T$) for isolated paramagnets; with eq 1, least-squares fits of several data sets establish that -7 cm$^{-1} \lesssim 2J \lesssim 6$ cm^{-1}. Thus these sites have been effectively uncoupled. The superexchange pathway which provides strong antiferromagnetic coupling in oxy and the other ≳90% met sites, therefore, is not present at the sites exhibiting these broad EPR signals. The endogenous exchange-mediating ligand appears to no longer bridge at the coupled binuclear copper site.

(16) It is difficult to directly quantify[17] this EPR signal as we are not certain that the entire signal is in the 0 to ~5000 G region and the EPR parameters are not accurately known. However, a calculation for the broad spectrum associated with met-Br$^-$ (pH = 5.7, 0.1 M acetate buffer and 0.1 M Br$^-$) (Results, section 2), which appears to be entirely in the 1000–5000-Gauss region, using g values from the best fit EPR spectral simulation (Results, section 3) showed that the signal corresponds to ~10% of the met sites.

(17) Aasa, R.; Vänngård, T. *J. Magn. Reson.* **1975**, *19*, 308–315.

(18) Beinert, H.; Orme-Johnson, W. H. In "Magnetic Resonance in Biological Systems"; Ehrenberg, A., Malmström, B. G., Vänngård, T., Eds.; Pergamon: Oxford, 1967; pp 221–247.

(19) The $g \approx 2$ signal appears as a direct result of the met preparation and, in contrast to sites exhibiting the broad signal, sites associated with this signal cannot be regenerated to the EPR-nondetectable oxy form.

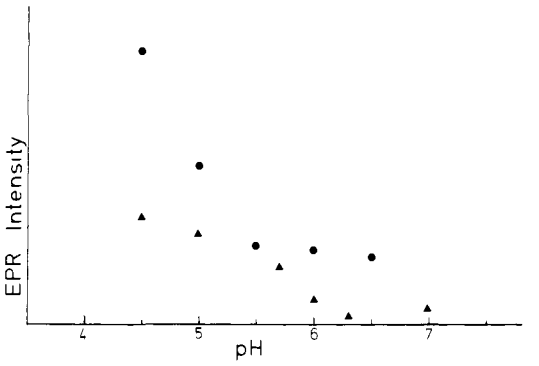

Figure 5. pH dependence of the broad met EPR signal intensity with 0.1 M acetate (▲) and 0.025 M azide (●); 1 mM protein. Relative signal intensity was determined by peak-to-peak height at $g > 4$ and peak height at $g = 2.22$, respectively.

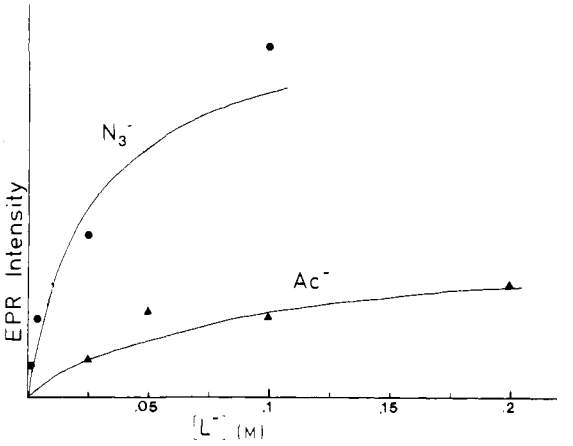

Figure 6. Plot of the broad met EPR signal intensity as a function of exogenous ligand concentration (1 mM protein): azide, 0.1 M MES at pH 5.5; acetate, 0.1 M succinate at pH 5.0. Relative signal intensity was determined as in Figure 5. Curves are least-squares fits of this data from plots of ΔI vs $\Delta I/[L^-]$; N_3^-, $K \simeq 40$ M^{-1}; Ac^-, $K \simeq 10$ M^{-1}.

Table I. Standardized Stability Constants for Anion Binding to the Unstable Met Hemocyanin Sites

pH	log $X_{1(Ac^-)}$[a]	log $X^*_{(Ac^-)}$[b]	log $X_{1(RO^-)}$[c]
6.0	1.81	0.0	1.81
5.7	1.80	0.60	1.20
5.5	2.34[d]	1.62 ± 0.4[d]	0.72[d]
5.3	1.76	1.38	0.38
5.0	1.70	1.32	0.38
5.0	1.70	2.43[e]	−0.73[e]
4.7	1.59	1.85	−0.26

[a] Calculated from eq 6 and $K_1 = 68$ M^{-1} and p$K_a = 4.56$.[24] [b] Experimentally measured. [c] Calculated from eq 8. [d] These data were determined by using the exogenous ligand azide; log $X_{1(N_3^-)}$ (column 1) was calculated by using $K_{1(N_3^-)} = 275$ M^{-1} and p$K_a = 4.92$.[24] [e] 0.05 M Cl$^-$ present.

2. Chemical Perturbations. The intensity of the broad EPR signal depends reversibly on both the pH and the concentration of specific exogenous anions. Figure 5 plots relative signal intensity in the presence of 0.1 M acetate[20] or 0.025 M azide[21] as a function of pH and shows that the signal becomes more intense as the pH is lowered. Figure 6 indicates the intensity of the EPR signal as a function of acetate or azide concentration at fixed pH; these data have been used[22] to determine the apparent binding constants

(20) Note that met EPR spectra presented prviously which show these signals have all been in acetate buffer.

(21) The azide EPR spectrum (see Figure 11) is quite different from that of acetate and is characterized by a broad feature at $g \simeq 2$ and a very weak feature at $g \simeq 4$. The azide signal intensity in Figures 5 and 6 is determined by monitoring the peak height at $g = 2.22$.

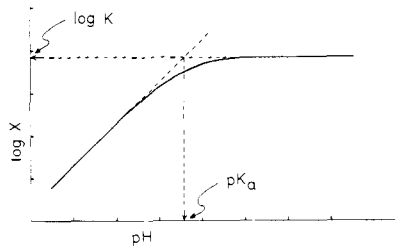

Figure 7. Theoretical plot of log standardized stability constant (X) vs. pH, indicating graphical determination of the log binding constant (K) and pK_a.

($X^*_{(L^-)}$) of Ac^- and N_3^- at various pH values (Table I, center). These chemical perturbations of the broad EPR signals are now interpreted as a pH-dependent, exogenous-ligand (acetate or azide), competitive displacement of the superexchange-mediating endogenous bridge at a small percentage of the met sites.

The endogenous bridge (RO^-) as well as exogenous ligands (L^-) have an intrinsic pK_a and a binding constant (K_l) at the binuclear cupric unit as shown in eq 2–5. Since L^- and, most likely, RO^-

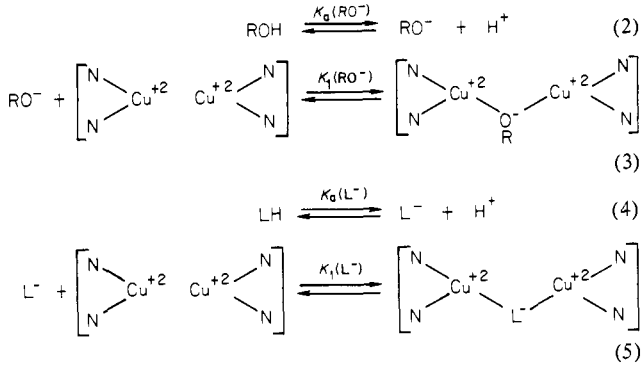

are weak acids, the binding constant will be pH dependent; we use the standardized stability value,[23] X_l, to describe this behavior (eq 6). A theoretical plot of log X_l vs. pH (Figure 7) graphically

$$X_{l(L^-)} = K_{l(L^-)} \frac{1}{1 + \frac{[H^+]}{K_{a(L^-)}}} \quad (6)$$

demonstrates this relationship and indicates how the values of log K_l and pK_a are determined. At a given pH, an apparent binding constant ($X^*_{(L^-)}$) for an exogenous ligand (L^-) is determined by experimentally monitoring the EPR signal from the species at the right side of eq 7. However, $X^*_{(L^-)}$ involves a competition of

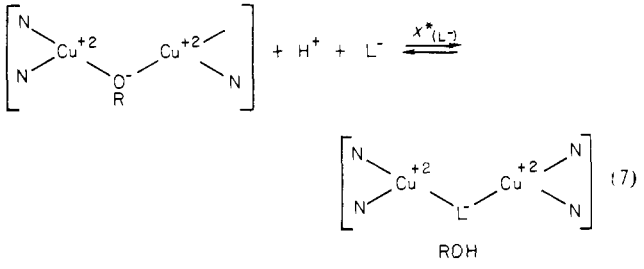

binding constants and can be reexpressed in terms of eq 2–5 with eq 8.

$$\log X^*_{(L^-)} = \log X_{l(L^-)} - \log X_{l(RO^-)} \quad (8)$$

We have used log $X^*_{(Ac^-)}$, determined by experimental data, and log $X_{l(Ac^-)}$, calculated from appropriate values for $K_{a(Ac^-)}$ (pK_a = 4.56) and $K_{l(Ac^-)}$ (68 M^{-1}),[24] to determine log $X_{l(RO^-)}$ (Table I). Figure 8 shows a pH plot of these values. Over the experimentally accessible pH range log $X_{l(RO^-)}$ is behaving as a linear function with slope $\simeq$ 1. This indicates that the experimental pH range is well below the bridge (RO^-) acidity constant (see Figure 7). The endogenous bridge in the protein site, therefore, is a protonatable residue with an intrinsic pK_a greater than 7.

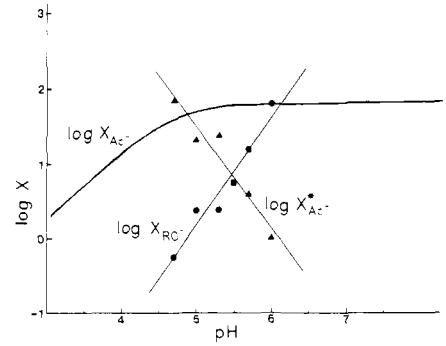

Figure 8. Plot of the data from Table I indicating log $X_{(Ac^-)}$ (—), log $X^*_{(Ac^-)}$ (▲), and log $X_{(RO^-)}$ (●); log $X_{(RO^-)}$ from competitive azide binding at pH 5.5 is also indicated (■). Straight lines are least-squares fits of the data points.

The strength of the superexchange coupling in the hemocyanin site limits the possible candidates for the endogenous bridge (i.e., imidazolate[25a] and other N donors do not appear to be reasonable possibilities). First-shell EXAFS data[25b,c] has further eliminated a sulfur ligand, and the above thermodynamic analysis eliminates carboxylate. This treatment, however, cannot directly distinguish between remaining high pK_a candidates: phenolate (tyrosine, pK_a $\simeq$ 10.7 in a hydrophobic environment), hydroxide (pK_a $\simeq$ 15.7), or alkoxide (serine or threonine, pK_a > 16). In Figure 8, the calculated values for log $X_{l(RO^-)}$ can be extrapolated to the pK_a's of these ligands in order to indicate their possible binding constants (tyrosine, log $K_l \approx 6$; hydroxide, log $K_l \approx 11$; serine or threonine, log $K_l \gtrsim 12$) at these binuclear cupric sites.[26]

While this analysis is only for the limited number of met sites which exhibit the broad EPR signals, it is shown in section 5 that these sites are capable of reversible oxygen binding and thus appear to contain the same endogenous bridge. Therefore, the intrinsic pK_a exhibited by the bridge in these sites should be appropriate for all met sites. The unique pH-dependent competitive anion behavior, however, is explained as a lower stability constant for the endogenous bridge in this limited number of sites relative to that in the other met sites.

In the absence of the competing ligands acetate or azide, EPR signals of uncoupled met sites are not observed down to pH $\simeq$ 4.5 (for pH < 4.5, there is an irreversible increase in $g \simeq 2$ intensity and the general protein reversibility becomes questionable). Therefore, the *apparent* pK_a of the bridging group in all sites must be <4.5.[27] Some literature data do exist[28] for the

(22) Byers, W.; Curzon, G.; Garbett, K.; Speyer, B. E.; Young, S. N.; Williams, R. J. P. *Biochim. Biophys. Acta* **1973**, *310*, 38–50.

(23) Sigel, H.; McCormick, D. B. *Acc. Chem. Res.* **1970**, *3*, 201–209.

(24) Martell, A. E.; Smith, R. M. "Critical Stability Constants"; Plenum: New York, 1977; Vol. 3.

(25) (a) Kolks, G.; Lippard, S. L.; Waszczak, J. V.; Lilienthal, H. R. *J. Am. Chem. Soc.* **1982**, *104*, 717–725. (b) Brown, J. M.; Powers, L.; Kincaid, B.; Larrabee, J. A.; Spiro, T. G. *Ibid.* **1980**, *102*, 4210–4216. (c) Co, M. S.; Hodgson, K. O.; Eccles, T. K.; Lontie, R. *Ibid.* **1981**, *103*, 984–986.

(26) Equation 3 has been written in a form which depends on [RO^-] and which describes a "stability constant" for the endogenous bridge at the binuclear cupric site. However, for a chelating protein residue, eq 3', which is

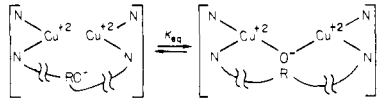

the expression describing an equilibrium between bound and unbound forms, is more appropriate. For the free ligand OH^-, $K_{l(RO^-)}$ does refer to a stability constant; however, for the endogenous protein bridge candidates, phenoxide and alkoxide, $K_{l(RO^-)}$ should be equated to K_{eq} of eq 3' (see: Sigel, H.; Scheller, K. H.; Reinberger, V. M.; Fischer, B. E. *J. Chem. Soc., Dalton Trans.* **1980**, 1022–1028).

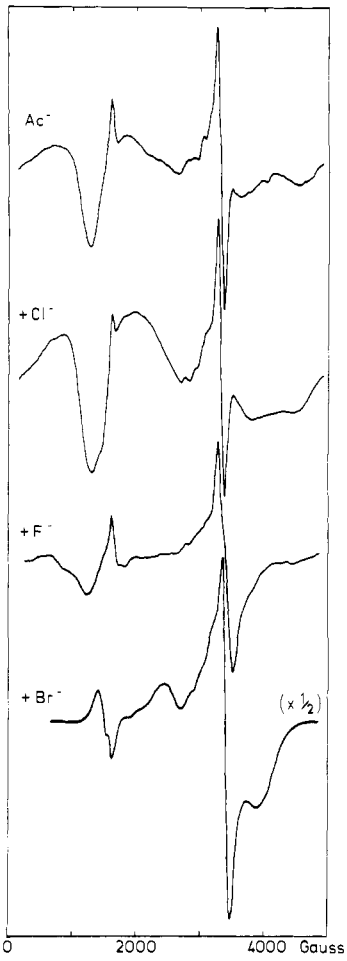

Figure 9. Met EPR spectrum (1 mM protein; 7 K) with 0.1 M acetate (pH 5.0), 0.1 M acetate (pH 5.0) + 0.1 M Cl^-, 0.1 M acetate (pH 5.0) + 0.1 M F^-, and 0.1 M acetate (pH 5.7) + 0.1 M Br^-.

apparent pK_a of bridging hydroxide in binuclear cupric model complexes; the value exhibited by these models (apparent $pK_a \approx 6$) is somewhat higher than that determined above.

Halide ions do not independently induce low pH signals in mollusc met hemocyanin. However, when added in the presence of acetate, they do modify the intensity and shape of the broad EPR signals (Figure 9). Fluoride decreases the signal intensity while chloride and bromide increase it. The different signals associated with chloride and bromide show that these exogenous anions are in fact binding at the site. Further, variation in the broad EPR signal intensity correlates with the electronegativities of the halides, indicating that these changes derive from an inductive effect.[29] This halide behavior can be explained through an extension of the above thermodynamic analysis. These ions appear to bind at the met site in the exogenous binding position and do not directly compete with the endogenous bridge for the endogenous binding position. They do, however, modify the stability constant of the endogenous bridge and thereby affect the extent of acetate competitive displacement of the bridge. In Table I (see data indicated by footnote *e*) we have quantitatively evaluated this halide inductive effect. When Cl^- binds in the exogenous position, it lowers the apparent stability constant of the endogenous bridge ($\Delta \log K_{1(RO^-)} = -1.11$) to a similar extent as found for mixed-ligand Cu(II) ternary complexes.[30]

Since low temperatures can affect the pH of buffered solutions and will modify stability constants, we have evaluated our data, obtained at temperatures down to ~7 K, with respect to these points. On the basis of a previous analysis[31] of freezing effects on the pH of buffered solutions, the buffers and protein concentrations used in this study should lead to negligible changes in pH upon cooling and freezing. Further, large increases in 7 K EPR signal intensities are observed with small changes in Cl^- or Br^- concentrations (5 mM halide vs. 1 mM protein); this behavior must relate to these anion effects and not modification of the pH upon cooling. Changes in stability constants with decreasing temperature have been addressed by performing the above thermodynamic calculation over a 2 order of magnitude range of log $K_{1(Ac^-)}$ values. The pH plot of log $X_{(RO^-)}$ is always found to be linear with slope ≈ 1 in the experimental range, indicating that temperature effects on stability constants do not affect our result that $pK_{a(RO^-)} > 7$.

3. Simulations. The broad EPR spectra from several of the chemically perturbed forms of met hemocyanin have been simulated in order to probe active site structural features. As the temperature dependence of these signals indicates there is negligible exchange coupling (section 1), dipolar interaction between the cupric ions is the dominant mechanism leading to zero field splitting (D) of the paramagnetic triplet spin state formed by the two $S = {}^1/_2$ ions (Figure 10, top). To first order, this dipolar zero field splitting is proportional to $1/r^3$, and the EPR spectrum should therefore reflect the Cu(II)–Cu(II) separation as schematically shown in Figure 10. However, when g anisotropy, hyperfine interaction, and lower site symmetry are also considered, the ion separation (r) cannot be directly determined from the powder EPR signals of dipolar coupled binuclear cupric complexes. Therefore, we have used an EPR spectral simulation calculation developed by Pilbrow[32] which is based on second-order perturbation analysis of a point-dipole model for anisotropic, binuclear $S = {}^1/_2$ systems when $|2J| \lesssim 30$ cm^{-1}. This calculation has been shown[33] to be capable of accurately determining the metal–metal separation in the range 3.5 to 4.0 Å and indicating the relative orientation of the magnetic axes on the two coppers; this program has also been used[8] to simulate the EPR spectrum of the dimer hemocyanin derivative where it was found that $r \simeq 6$ Å.

Simulations of the broad dipole-coupled EPR signals associated with met are shown in Figure 11, and the best fit simulation parameters are indicated in Table II. We find that the EPR signals in Figure 11 reflect dramatic differences in Cu(II)–Cu(II) separation: N_3^-, $r = 5.0$ Å; Br^-, $r = 2.9$ Å; Ac^-, $r = 2.4$ Å. The unrealistically small value of $r = 2.4$ Å for the acetate signal

Table II. Best Fit Simulation Parameters for EPR Spectra from Chemically Perturbed Unstable Met Sites

	acetate and acetate + Cl^-	acetate + Br^-	N_3^-
r, Å	2.4 ± 0.1	2.92 ± 0.05	5.0 ± 0.2
ξ, deg[a]	60	90	85
$g_\parallel$	2.05	2.12	2.15
$g_\perp$	2.25	2.01	2.07
$A_\parallel$, $\times 10^4$ cm^{-1}	150	150	120
$A_\perp$, $\times 10^4$ cm^{-1}	20	20	25
$\lvert 2J \rvert$, cm^{-1}	1.0 ± 5.0	0.0 ± 5.0	0.0 ± 5.0

[a] $\eta = 0°$, $\alpha = 0°$ (see ref 32).

(27) Since the apparent pK_a reflects a competition between H^+ and the metal ion site, this value is merely the difference between the intrinsic pK_a and log $K_{1(RO^-)}$. The upper limit of the apparent pK_a (<4.5), therefore, provides another method for determining the stability constants of the three bridge candidates (tyrosine, log $K_1 > 6$; hydroxide, log $K_1 > 11$; serine or threonine, log $K_1 > 12$). These values compare well with those determined by extrapolating the competitive anion thermodynamic analysis and indicate internal self-consistency in the treatment of our experimental data.

(28) (a) Coughlin, P. K.; Lippard, S. J. *J. Am. Chem. Soc.* **1981**, *103*, 3228–3229. (b) Burk, P. L.; Osborn, J. A.; Youinou, M. -T.; Agnus, Y.; Louis, R.; Weiss, R. *Ibid.* **1981**, *103*, 1273–1274. (c) Motekaitis, R. J.; Martell, A. E.; Lecomte, J. -P.; Lehn, J. -M. *Inorg. Chem.* **1983**, *22*, 609–614.

(29) The fact that oxy hemocyanin does not exhibit these broad EPR signals appears to relate to the high electronegativity of O_2^{2-} bound at the met site in oxy.

(30) Sigel, H.; Griesser, R.; Prijs, B. *Z. Naturforsch. B: Anorg. Chem. Org.* **1972**, *27B*, 353–364.

(31) Williams-Smith, D. L.; Bray, R. C.; Barber, M. J.; Tsopanakis, A. D.; Vincent, S. P. *Biochem. J.* **1977**, *167*, 593–600.

(32) Smith, T. D.; Pilbrow, J. R. *Coord. Chem. Rev.* **1974**, *13*, 173–278.

(33) Boyd, P. D. W.; Toy, A. D.; Smith, T. D.; Pilbrow, J. R. *J. Chem. Soc., Dalton Trans.* **1973**, 1549–1563.

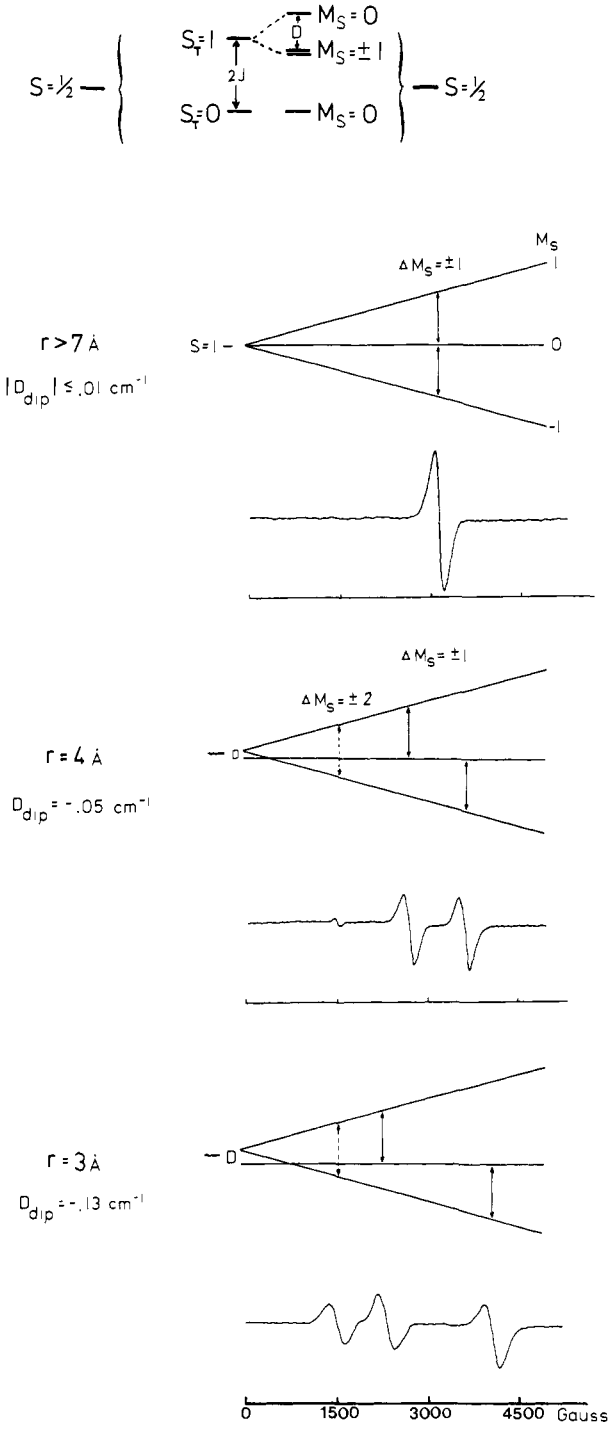

Figure 10. (Top) Singlet and triplet total spin states (S_T) formed by two $S = 1/2$ ions; exchange splitting ($2J < 0$) and zero field splitting (D) for $H \| r$ are indicated; (bottom) splitting of the triplet ($S_T = 1$) energy levels in a magnetic field ($H \perp r$), Zeeman transitions and associated EPR spectra for axial ($\xi = 0°$) isotropic ions (hyperfine not included) at $\gtrsim$7- (upper), ~4- (middle), and ~3-Å (lower) separation. Note for $D < {}^1/_2 h\nu$ appreciable $\Delta M_s = \pm 2$ intensity is only found for H not parallel to the principal axes, and therefore these EPR spectra represent all orientations of a powder sample.

indicates that both the second-order perturbation analysis and the point-dipole model are breaking down due to comparable magnitudes of the zero field splitting and the microwave energy, the close approach of the cupric ions, and/or possible contributions from anisotropic exchange interaction.[34] This signal does, however, reflect a shorter Cu–Cu separation than that of the Br^- signal. The g and A values used in simulating the Br^- and N_3^- signals are appropriate for two tetragonal cupric ions, and the best fit angle ξ (defined at the top left of Figure 11) indicates that the unique g tensor axis of each ion is oriented approximately perpendicular to the internuclear vector. A large number of simulations, however, have shown that the broad line widths and lack of hyperfine structure in the experimental spectra do not allow us to achieve a high degree of accuracy for the simulation parameters ξ, $g_{x,y,z}$, and $A_{x,y,z}$. Alternatively, simulations of the Br^- and N_3^- spectra were quite sensitive to small changes in r leading to a high degree of confidence in this parameter.

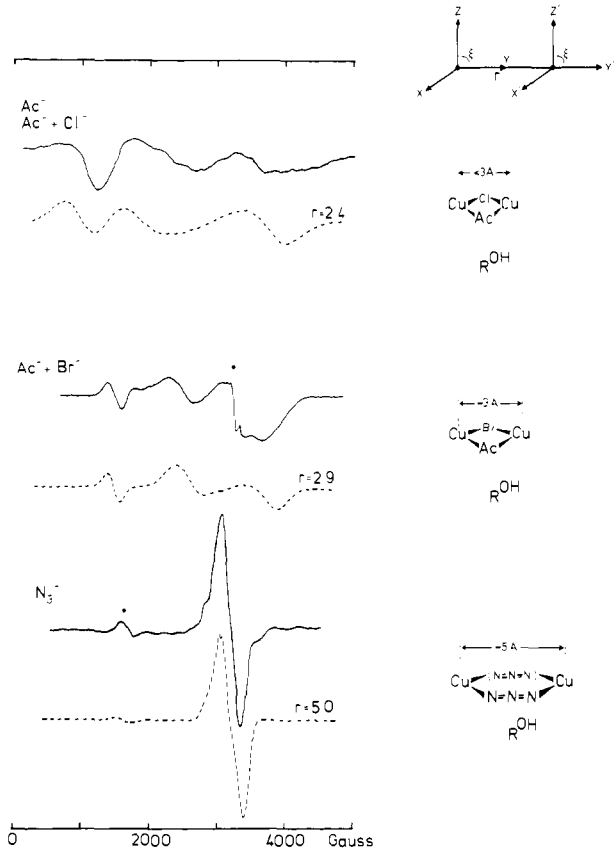

Figure 11. (Left) 7 K met hemocyanin EPR signals (—) and best fit simulations (---) using parameters listed in Table II; $g \simeq 4.3$ iron and $g \approx 2$ mononuclear cupric signals have been removed from the experimental spectra (★ indicates subtraction discrepancies). (Right) (top) Orientation of the principal g tensor axes with respect to r ($\xi = 90°$ in this orientation); (lower) structural representation of sites exhibiting these EPR signals.

These simulations have indicated that when the endogenous bridge is uncoupled, exogenous anions modify the Cu–Cu distance. Since the relative metal ion separation correlates with the ionic radii of the halides and their expected bridging distances, this trend supports a bridging geometry for Cl^- and Br^- coordinated at the exogenous ligand binding site. The metal–metal separation determined for these two signals is short enough ($r < 3.1$ Å) to sustain a unidentate or bidentate bridging mode for acetate, which competes with the endogenous bridge for the endogenous binding site. The $r \approx 5$ Å determined from the azide signal clearly requires a μ-1,3 bridging geometry for this ligand. Though these exogenous anions are tightly bound and bridge the copper ions, they do not mediate significant exchange coupling ($|2J| < 7$ cm^{-1}); poor overlap must therefore exist between the bridging ligand orbitals involved in the superexchange pathway and at least one of the Cu(II) $d_{x^2-y^2}$ valence orbitals. The structural information determined by simulation of these EPR signals is summarized in the active site representations shown on the right side of Figure 11.

4. Comparison of Arthropod and Mollusc Met Hemocyanins. During the arthropod met reaction with azide (Figure 12), an

(34) Banci, L.; Bencini, A.; Gatteschi, D. *J. Am. Chem. Soc.* **1983**, *105*, 761–764.

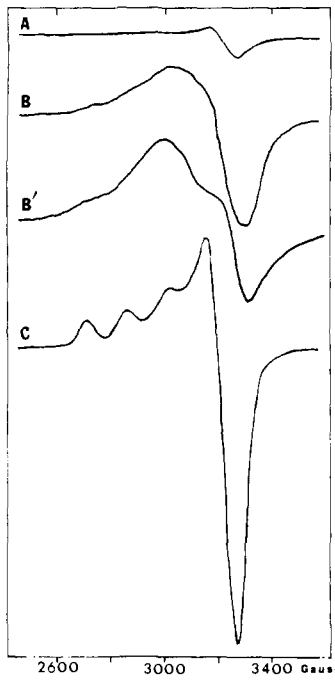

Figure 12. EPR spectra of *Cancer* met hemocyanin (0.1 M phosphate at pH 6.3; 77 K, ν = 9.08 GHz) 0 (A), 5 (B), and 180 (C) min after addition of 50-fold excess azide; (B′) *Busycon* met hemocyanin (0.1 M acetate at pH 5.0; 7 K, ν = 9.45 GHz) with 0.1 M azide; spectrum B′ is normalized to match resonance conditions and signal intensity of A–C.

intermediate broad $g \approx 2$ signal (Figure 12B) is observed[6,35] before the irreversible appearance of a ~35% mononuclear cupric signal (Figure 12C). While the other ~65% of the sites remain in the EPR-nondetectable met form, the behavior of this ~35% has been described[35] as a "springing" of the binuclear cupric site.[36] This broad $g \approx 2$ intermediate feature can be stabilized[16] at low azide concentrations and pH >7; it is very similar to that exhibited by the mollusc sites reversibly uncoupled by azide (Figure 12B′). If the arthropod met reaction with azide is stopped at this intermediate stage through removal of the anion by dialysis, this broad $g \simeq 2$ signal is lost, and the very weak EPR signal associated with the original met (Figure 12A) returns.

The irreversible $g \simeq 2$ EPR signal associated with arthropod met has pH and anion dependent behavior which parallels the reversible broad EPR signals associated with mollusc met (Section 2). In 0.1 M acetate, the $g \simeq 2$ signal intensity of *Cancer* met exhibits pH dependence very similar to that shown in Figure 5 for mollusc met. Further, analogous to the mollusc met behavior shown in Figure 9, Cl^- increases this signal intensity at each pH value until the ~35% maximum intensity is reached. *Limulus*, which has been found[6] to have somewhat different chemical behavior and spectroscopic features than other arthropods and which has been reported[5,6,37] to not exhibit the met $g \simeq 2$ EPR signal when treated with excess azide, was also investigated. Similar irreversible $g \simeq 2$ EPR signals were found for *Limulus* met in the extended pH range of this study. Although these signals show behavior analogous to other arthropods, they occur at a somewhat lower pH (0.1 M acetate, pH <5.5). Parallel to mollusc results shown in Figure 9, fluoride prevents these low pH *Limulus* met signals, while chloride, bromide, and azide induce the full 30–35% signal intensity.

Parallel chemical behavior and spectral features (Figure 12B and B′) allows the ~35% arthropod met sites, which are unstable to displacement of the endogenous bridge, to be correlated with those found in the molluscs. However, as indicated in Scheme I, when exogenous anions competitively displace the endogenous bridge in the unstable fraction of arthropod met, the binuclear cupric site is irreversibly disrupted. Apparently the endogenous bridge is required[38] to stabilize the arthropod binuclear copper met site. Only azide replaces the endogenous bridge to form a metastable uncoupled site intermediate (Scheme I), bridging the coppers at a ~5-Å separation prior to the irreversible active site disruption (Cu–Cu separation ≳ 7 Å).

Scheme I. Representation of the Arthropod Met Hemocyanin Active-Site Instability

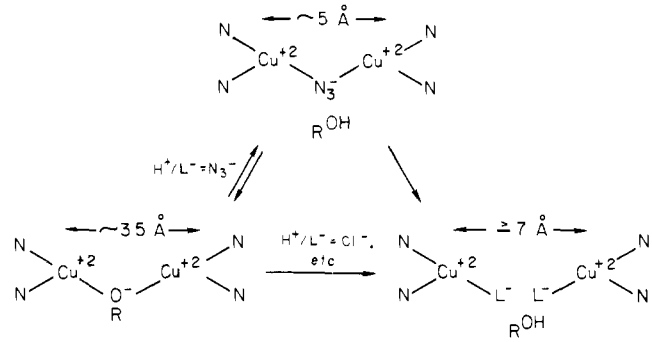

5. Nature of the Active-Site Instability. The chemistry developed in section 2 allowed us to perform the following experiment which establishes the validity of the fraction of met sites exhibiting this active-site instability. Mollusc met hemocyanin, which exhibits the broad EPR signals at pH 5.0 (0.1 M acetate buffer), can be dialyzed to high pH (>7.0) where these signals are absent. Treatment with peroxide then leads to ≳95% regeneration to oxy; the broad EPR signals do not appear upon dialysis to the original low pH conditions. All sites now function normally in reversible oxygen binding. If this same protein is then subjected to a second met preparative procedure, the broad EPR signals quantitatively reappear at pH 5.0 (0.1 M acetate buffer). This indicates that the unstable met sites are not irreversibly damaged sites but are in fact binuclear copper sites which function normally in reversible oxygen binding. Further, this result implies that these sites have geometric and electronic structural features similar to other hemocyanin sites and allows us (section 2) to correlate specific features of these sites (i.e., pK_a of the endogenous bridge) with those of normal sites.

This instability of a limited number of met sites is not due to damage induced by the met preparation, as neither longer met preparation conditions nor a mollusc "cycling" procedure (alternating met preparation and peroxide regeneration to oxy) leads to an increase in the number of sites exhibiting competitive uncoupling behavior. The limited nature of this instability is also not associated with active-site accessibility by exogenous anions since N_3^- will displace peroxide from oxy to generate >90% met sites which exhibit the ~35% (arthropod) and ≲10% (mollusc) uncoupled site EPR signals.

Results do, however, indicate that this limited instability is associated with a specific heterogeneous component of the active sites. In the case of mollusc hemocyanin, peroxide regeneration of *Busycon* met at low pH, where the unstable sites are uncoupled, leads to ≳90% oxy protein with the remaining ≲10% met still uncoupled and EPR detectable;[39] we designate this protein form as oxy′. Alternatively, a protein which contains ~90% oxy and ~10% met sites can be prepared by terminating the met prepa-

(35) McMahill, P. E.; Mason, H. S. *Biochem. Biophys. Res. Commun.* **1978**, *84*, 749–754.

(36) A binuclear cupric site which exhibits a "mononuclear" signal must have negligible exchange coupling and a Cu(II)–Cu(II) separation ≳7 Å.

(37) Lijnen, H. R.; Witters, R.; Lontie, R. *FEBS Lett.* **1978**, *88*, 358–360.

(38) A parallel requirement for stabilization of the arthropod binuclear copper site has been found in metal removal studies; apparently both metal ions are required to form the site since removal of the second ion is nearly an order of magnitude faster than removal of the first.[6] While the mollusc active site appears to be well formed (stabilized during metal removal and endogenous bridge uncoupling), arthropod hemocyanin seems to require the endogenous bridge and both metal ions to form the active site.

(39) Binding of peroxide by *Busycon* met hemocyanin thus requires that the site be coupled by the endogenous bridge; apparently this is not the case for *Helix pomatia*.[40]

(40) Deleersnijder, W.; Witters, R.; Lontie, R. *Life Chemistry Reports Supplement 1* **1983**, 289–290.

Table III. Met Active Site Instability in the Heterogeneous Fractions of *Limulus polyphemus* Hemocyanin

fraction	% of protein[a]	heterogeneity[a]	% of unstable[b] met sites
I	14.8	I, I', I''	42
II	20.5	II, II', II'', IIa, IIa'	41
III	30.6	IIIa, IIIb, IIIb'	25
IV	19.7	IV	62
V	14.4	V, V', VI	10
whole protein	100.0		36[c]

[a] Reference 14; heterogeneity determined by electrophoresis. [b] ≤10% sites damaged during prep; ≤20% residual oxy. [c] Weighted average of individual fraction instability.

rative procedure[10] after ~15 min rather than 48 h. This latter sample exhibits only very weak uncoupled-site EPR signals (~$^1/_{10}$ that of oxy') which increase in direct proportion to the amount of met produced as the preparation is allowed to continue. Comparison of the two protein forms with ~90% oxy and ~10% met indicates that the active-site instability does not relate to an equilibrium percentage of all met sites but is associated with a specific subset of the met sites. Under conditions of cooperative O_2 binding by hemocyanin,[41] the broad EPR signal is not affected when the ~90% oxy sites of oxy' are pumped to deoxy;[42] thus, intersite interactions associated with changes in the protein quaternary structure dot not appear to correlate with the fraction of unstable met sites. In arthropod hemocyanin we have been able to probe the unstable met sites by chromatographically separating[14] the five heterogeneous fractions of *Limulus* hemocyanin. As indicated in Table III, we find that the four fractions which display further electrophoretic heterogeneity[14] contain various percentages of the unstable met sites. However, nearly all the sites of the one homogeneous fraction (**IV**) exhibit this active-site instability. The arthropod met instability thus appears to correlate with specific electrophoretically heterogeneous components.

Protein tertiary structure appears to be dictating this active-site instability in a heterogeneous fraction of the met hemocyanin sites. This instability could derive from steric strain imposed by protin folding on the endogenous bridge or from differences in hydrophobic interactions within the active site pocket. Both of these effects could modify the stability constant of the endogenous protein bridge.

Finally, we note that low-temperature (~7 K) EPR studies of resting (met) *Neurospora crassa* tyrosinase at pH 5.0 with Ac^-, Cl^-, and N_3^- fail to reveal any features indicative of uncoupled sites. This enzyme, which is homogeneous by electrophoresis,[44] has coupled binuclear copper active sites that have been shown to be extremely similar to those of hemocyanin[45] and that appear to chemically parallel the ≳90% mollusc and ~65% arthropod met hemocyanin sites which remain EPR nondetectable under these reaction conditions.

Summary

Previously it has been shown[4] that the EPR signals associated with mollusc met hemocyanin originate from a small fraction of the active sites. This study demonstrates that these broad signals, most obvious at $g > 4$, are due to met sites where the antiferromagnetic superexchange coupling has been reversibly eliminated. Chemical perturbations further show that these are not damaged sites but binuclear copper protein units which can be regenerated to function normally in reversible oxygen binding. Therefore they exhibit certain intrinsic properties of the coupled binuclear copper active site.

This study has shown that a pH-dependent competitive displacement of the endogenous bridge by certain exogenous anions (acetate and azide) reversibly eliminates the strong exchange coupling in these sites. This gives rise to EPR signals of the binuclear cupric triplet spin state which is perturbed by dipolar interaction between the Cu(II)'s. At pH 5.0, 0.1 M acetate, and 50 mM Cl^-, 10 ± 5% of the mollusc met sites are thus uncoupled. Simulation of these zero-field-split triplet EPR signals indicates that the exogenous anions now determine the Cu(II)–Cu(II) separation by bridging the metal ions in these dipolar interacting ($|2J| \lesssim 7$ cm^{-1}) sites. The competitive displacement in these unique sites has been quantitatively described as being due to a larger stability constant for the exogenous anion than for the endogenous bridge in the pH range where the signals are observed. This behavior thus appears to arise from a lower stability constant for the endogenous bridge at these met sites relative to other coupled binuclear copper active sites. Although the halides do not compete with the endogenous bridge, they do bind at the site and inductively modify the bridge stability constant leading to increased or decreased site uncoupling. Computer simulation of these EPR signals shows that the halide ions also modify the Cu(II)–Cu(II) separation in these dipolar interacting sites. This is clear evidence that the coupled binuclear copper active site has two distinct bridging coordination positions, an endogenous one and an exogenous one. With respect to this bridging ligation, the parameters used to simulate the EPR spectra indicate a picture of these uncoupled sites which parallels the spectroscopically effective oxy hemocyanin active site (Figure 1).

The limited nature of this active-site instability is not due to different site accessibility but rather to a specific heterogeneity[46] of this small percentage of active sites. This heterogeneity appears to relate to tertiary protein effects that lower the stability constant of the endogenous bridge and could be due to a specific steric strain on the bridge or a different hydrophobic environment of these unique active sites. The met instability in arthropods quantitatively accounts for ~35% of the active sites. In this phyla, however, the competitive pH-dependent reaction with exogenous anions leads to an irreversible uncoupling of these sites. Additional structural features must be present which lead to the irreversibility and ≳7 Å Cu(II)–Cu(II) separation when these arthropod met sites are uncoupled.

The thermodynamic analysis used in this study has indicated that the endogenous bridge in these unstable sites has an intrinsic $pK_a > 7$. As these sites function normally in reversible oxygen binding they must have an active-site structure very similar to that of normal sites. A different endogenous bridge is thus excluded as the basis of this instability, and the intrinsic pK_a of the bridge determined in this study is characteristic of all hemocyanin sites. Therefore, carboxylate and other low pK_a bridging ligand candidates are eliminated, and tyrosine, hydroxide, serine, and threonine emerge as likely possibilities for this bridging unit. The apparent pK_a required by this analysis for bridging hydroxide, however, appears to be smaller than is found for known μ-OH^- binuclear cupric model complexes.

A band at 425 nm in the optical absorption spectrum of both met and oxy hemocyanin may be associated with the endogenous bridge.[1,3] EXAFS results have shown that this feature cannot be due to a tightly bound sulfur ligand.[25b,c] Table IV of ref 47 has compiled exchange coupling and optical absorption data for well-characterized binuclear cupric model complexes containing bridging phenoxide, hydroxide, and alkoxide ligands. While all

(41) Mangum, C. P.; Lykkeboe, G. *J. Exp. Zool.* **1979**, *207*, 417–430.
(42) This behavior should be compared to that of the spectral probe derivative[43] which has a small percentage of EPR-detectable half met sites dispersed in oxy hemocyanin. When this protein is deoxygenated, the EPR signals exhibit dramatic changes which relate to the intersite interaction associated with changes in quaternary protein structure.
(43) Hwang, Y. T.; Solomon, E. I. *Proc. Natl. Acad. Sci. U.S.A.* **1982**, *79*, 2564–2568.
(44) Lerch, K. *FEBS Lett.* **1976**, *69*, 157–160.
(45) Himmelwright, R. S.; Eickman, N. C.; LuBien, C. D.; Lerch, K.; Solomon, E. I. *J. Am. Chem. Soc.* **1980**, *102*, 7339–7344.
(46) It should be noted that within the biochemical heterogeneous fraction described in this study there is a further spectroscopic heterogeneity that originates from the relatively low energy of residue interactions in protein folding. This can lead to a distribution of sites resulting in inhomogeneously broadened EPR linewidths.
(47) Solomon, E. I.; Penfield, K. W.; Wilcox, D. E. In "Structure and Bonding"; Clarke, M. J., et al., Eds.; Springer-Verlag: Berlin, 1983; Vol. 53, pp 1–57.

three candidates are capable of mediating the strong superexchange interaction found in the coupled binuclear copper site and all three have charge transfer to copper(II) optical features in the 300–500-nm region, the more likely assignment of this 425-nm band, based on known[48] model complexes, appears to be a phenolate-to-copper CT transition.

This study clarifies and supports certain aspects of the spectroscopically effective picture of the coupled binuclear copper active site in hemocyanin (Figure 1). It has shown that the endogenous bridge can be reversibly protonated and displaced, eliminating the strong superexchange coupling, and that there are two distinct and different binding positions, one for the endogenous bridging ligand and a second for exogenous bridging ligands.

Acknowledgment. We are grateful to NIH, Grant AM31450, for support of this research. We thank John Pilbrow for providing the EPR simulation program GNDIMER, Roy Planalp and Luke Schoeniger for technical assistance, and Arturo Porras, David Richardson, Harvey Schugar, and Darlene Spira for helpful discussions.

Registry No. N_3^-, 14343-69-2; Cl^-, 16887-00-6; Br^-, 24959-67-9; copper, 7440-50-8; acetic acid, 64-19-7; fluoride, 16984-48-8; oxygen, 7782-44-7.

(48) (a) Amundsen, A. R.; Whelan, J.; Bosnich, B. *J. Am. Chem. Soc.* **1977**, *99*, 6730–6739. (b) Ainscough, E. W.; Bingham, A. G.; Brodie, A. M.; Husbands, J. M.; Plowman, J. E. *J. Chem. Soc., Dalton Trans.* **1981**, 1701–1707.

Tricyclo[4.2.2.2^{2,5}]dodeca-1,5-diene

Kenneth B. Wiberg,* Michael G. Matturro, Paul J. Okarma, and Mark E. Jason

Contribution from the Department of Chemistry, Yale University, New Haven, Connecticut 06511. *Received October 26, 1983*

Abstract: Tricyclo[4.2.2.2^{2,5}]dodeca-1,5-diene (**1**), the simplest member of the series of "superphanes", has been prepared by the dimerization of bicyclo[2.2.0]hex-1(4)-ene. The structure of **1** was determined by X-ray crystallography, giving a distance between the double bonds of 2.40 Å. The mechanism of the dimerization is discussed, and the energies of the intermediates are estimated by a combination of ab initio geometry optimizations and molecular mechanics calculations. The properties of **1** are discussed with special emphasis on the interaction between the double bonds. The reactions, including the Cope rearrangement to 2,5-dimethylenetricyclo[4.2.2.0^{1,6}]decane, epoxide formation, and transannular bridging on reaction with bromine are described.

The relative importance of through-bond and through-space interactions[1] has received much study, particularly with regard to interacting π-electron systems in compounds such as norbornadiene,[2] bicyclo[2.2.2]octa-2,5-diene,[2] and the cyclophanes.[3] In this connection, tetracyclo[4.2.2.2^{2,5}]dodeca-1,5-diene (**1**) is

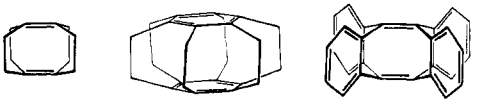

1 **2** **3**

of special interest since the two double bonds are forced to interact strongly and since it may be considered to be the simplest analogue of superphane (**2**).[4] A tetrabenzo derivative, **3**, has been reported,[5] and it was found that the repulsion between the double bonds led to pyramidalization with an out of plane bending angle of 30.6°. We have been able to prepare **1** by the dimerization of bicyclo[2.2.0]hex-1(4)-ene (**4**) in dilute solution.[6] We now report the details of its formation, along with information on its properties and its reactions.

When **4** was allowed to remain in dimethylformamide or pentane solution at around room temperature, it was found to slowly disappear. If the concentration were relatively high (>0.01 M), the major product was an insoluble polymer. However, using a dilute solution (0.002 M), relatively little polymer was formed, and the main product was **1**. Some of the exocyclic diene **5** also was formed.

Table I. Kinetics of Dimerization of Bicyclo[2.2.0]hex-1(4)-ene Bicyclo[2.2.0]-hex-1(4)-ene (3)[a]

T, °C	10^2k, L mol^{-1} s^{-1}
0.0	1.13 ± 0.06
20.8	3.79 ± 0.20
39.0	19.3 ± 0.9
59.5	53.7 ± 2.7

[a] $\Delta H^{\ddagger}$ = 11.5 ± 0.5 kcal/mol, $\Delta S^{\ddagger}$ = −25 ± 2 eu.

Scheme I

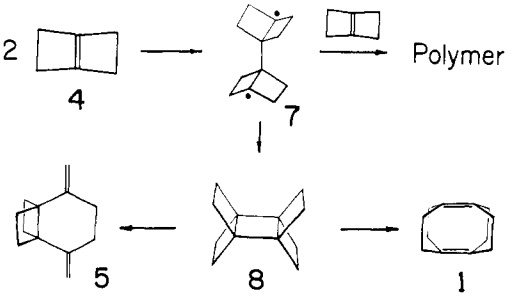

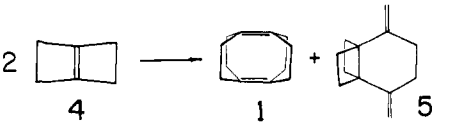

(1) Hoffmann, R. *Acc. Chem. Res.* **1971**, *4*, 1.
(2) Heilbronner, E.; Maier, J. P. In "Electron Spectroscopy"; Brundle, C. R., Baker, A. D., Eds.; Academic Press: New York, 1977; Vol. I, p 205.
(3) Kovac, B.; Mohranz, M.; Heilbronner, E.; Boekelheide, V.; Hopf, H. *J. Am. Chem. Soc.* **1980**, *102*, 4314.
(4) Sekine, Y.; Boekelheide, V. *J. Am. Chem. Soc.* **1981**, *103*, 1777.
(5) Viavattene, R. L.; Greene, F. D.; Cheung, L. D.; Majeste, R.; Trefonas, L. *J. Am. Chem. Soc.* **1974**, *96*, 4342.
(6) Wiberg, K. B.; Matturro, M.; Adams, R. *J. Am. Chem. Soc.* **1981**, *103*, 1600.

0002-7863/84/1506-2194$01.50/0